

Post Print

Resonant Photoemission at the 2p Edges of Ni: Resonant Raman and Interference Effects

M. Weinelt, A. Nilsson, Martin Magnuson, T. Wiell, N. Wassdahl, O. Karis, A. Föhlisch,
N. Mårtensson, J. Stöhr and M. Samant

N.B.: When citing this work, cite the original article.

Original Publication:

M. Weinelt, A. Nilsson, Martin Magnuson, T. Wiell, N. Wassdahl, O. Karis, A. Föhlisch,
N. Mårtensson, J. Stöhr and M. Samant, Resonant Photoemission at the 2p Edges of Ni:
Resonant Raman and Interference Effects, 1997, Physical Review Letters, (78), 5, 967-970.

<http://dx.doi.org/10.1103/PhysRevLett.78.967>

Copyright: American Physical Society

<http://www.aps.org/>

Postprint available at: Linköping University Electronic Press

<http://urn.kb.se/resolve?urn=urn:nbn:se:liu:diva-17473>

Resonant Photoemission at the $2p$ Edges of Ni: Resonant Raman and Interference Effects

M. Weinelt, A. Nilsson, M. Magnuson, T. Wiell, N. Wassdahl, O. Karis, A. Föhlisch, and N. Mårtensson

Department of Physics, Uppsala University, P.O. Box 530, S-751 21 Uppsala, Sweden

J. Stöhr and M. Samant

IBM Research Division, Almaden Research Center, 650 Harry Road, San Jose, California 95120

(Received 21 October 1996)

Unambiguous evidence for resonant photoemission in Ni is presented. Interference effects are identified at the $2p$ edges for the valence band and the 6 eV satellite. A rapid transition from a resonant Raman to an Auger-like regime shows that the core-excited states above threshold are not localized enough to significantly enhance the photoemission intensity, implying a large fraction of incoherent intensity. The results indicate that the appearance of interference effects does not require strong localization of the intermediate state. [S0031-9007(97)02315-6]

PACS numbers: 79.60.Bm, 33.60.Fy, 71.27.+a

Resonant photoemission is a powerful tool for electronic structure studies [1], e.g., of lanthanides, actinides, and $3d$ -transition metals, notably in recent years the $3d$ -metal oxides. It has been used to locate the $4f$ states in the early lanthanides and correlation satellites in $3d$ -metal systems. There is rapid progress in the field due to the development of new high-resolution beam lines capable of reaching also the deeper core edges of the transition metals. The field has also been stimulated by recent progress in high-resolution gas-phase studies [2,3] as well as the related technique of resonant inelastic x-ray scattering [4]. In order to use the full potential of these powerful electronic structure techniques, it is essential to have a solid understanding of the resonance process.

Ni is a prototype system for resonant photoemission. Guillot *et al.* [5] observed a strong enhancement of the 6 eV valence-band satellite at the $3p$ threshold. This result was explained as due to a $3p$ to $3d$ excitation followed by a Super-Coster-Kronig decay to a $3d$ double-hole state, i.e., the same type of state as the photoemission satellite. If the states are identical, the two channels interfere, leading to Fano profiles [6] for the photon-energy dependence of the intensity. Resonance effects were also reported for the normal valence-band emission [7]. The resonant behavior of Ni has been further studied by angle-dependent [8] and spin-polarized photoemission [9].

The theoretical models have focused on the presence of unfilled d states and an atomiclike core-excited intermediate state. The photoemission spectrum of Ni has been treated within the Hubbard model [10,11] or in terms of configuration interaction states built from atomic configurations [12]. To explain the fact that similar resonances were observed also in Cu, which has a formally filled d band, an alternative mechanism was proposed [11] in which the resonance is maintained by the many-body properties of the core-excited states close to threshold.

In recent years, the concept of resonant photoemission has been much discussed [8,13–15] for the $3d$ -metal

systems, especially for the metals themselves. Based on comparisons with lanthanide systems, measurements of angular distributions, and on considerations of the resonance profiles, it has been argued that the core-excited intermediate states are not localized enough to allow the resonance processes to occur. It has been proposed instead that the resonantly enhanced photoemission satellite in Ni is due to incoherent Auger processes which are enhanced at the same photon energies due to the strong absorption just above the core edge [8,13,14].

We address this controversial issue based on measurements at the $2p$ edges of Ni. Most previous investigations have been performed at the much shallower $3p$ thresholds where the results are less transparent due to other photon-energy dependent effects such as rapidly varying atomic transition matrix elements and direct transitions relating to the k -dependent band structure. There are also complications due to overlapping spin-orbit split edges, possible core-valence couplings and rapid Coster-Kronig processes producing broad resonances. At the $2p$ thresholds, many of these problems are less severe. The large $2p$ spin-orbit splitting even makes it possible to compare the behavior at the two edges separately, thereby exploring the consequences of a competing Coster-Kronig channel at the $2p_{1/2}$ threshold. Finally, we have used the different angular dependencies for the direct and core-assisted processes to vary their relative weights by varying the polarization of the incoming beam. We show that many of the previous conclusions concerning the resonance effects in the $3d$ transition metals have to be refined. We present unambiguous evidence for resonant photoemission. However, incoherent processes are important as well, and the results show that one has to be more precise in the definition of the resonant phenomena and that one has to distinguish between different photon-energy regimes.

The experiments were made using a Ni(100) crystal at beam line 8.0 at the Advanced Light Source. This undulator beam line is equipped with a modified “Dragon”

monochromator. The end station was built at Uppsala University and comprises a rotatable Scienta SES200 electron spectrometer [16]. The measurements were performed at high resolution in the incident and exit channels (150 meV each). This capability allows us to exploit the concept of the Auger resonant Raman effect [2]. The spectra were recorded at normal emission with the \mathbf{E} vector of the x rays in the plane of the sample or normal to it (achieved by rotating both sample and spectrometer). The latter geometry enhances the relative weight of the photoemission matrix element. We denote these the ‘‘Auger’’ and ‘‘photoemission’’ geometries, respectively.

The term resonant photoemission has been used in different ways. We can distinguish three criteria for resonant photoemission: (i) There are intensity modifications (usually an enhancement) of the photoemission states at a core-level threshold due to core-hole assisted processes. (ii) A resonant photoemission feature has to appear at constant binding energy. In terms of the Auger channel, this is the resonant Raman effect. (iii) There is interference between the different channels yielding intensities which are not simply the sum of the intensities of the individual subprocesses.

Figure 1 compares a set of valence electron spectra recorded for photon energies around the L_3 threshold at 852.3 eV. The kinetic energy is given relative to the Fermi level and hence the photon energy corresponds to the high energy cutoff in each spectrum. The results are shown for the Auger (dashed line) and photoemission geometries (solid line). Starting with the spectra below resonance we see two types of states, bandlike states within 2.3 eV from the Fermi level which dominate the spectra and split-

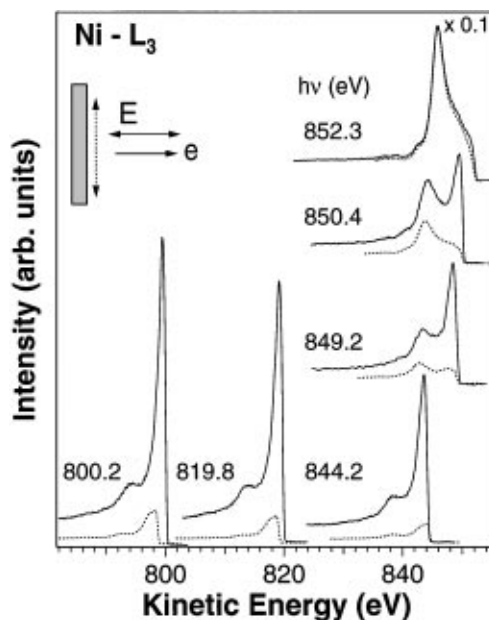


FIG. 1. Valence electron spectra recorded around the Ni L_3 threshold. The \mathbf{E} vector of the incident x rays is in the surface plane (dashed line) or perpendicular to it (solid line).

off atomiclike $3d^8$ satellite states at 6 eV. The intensities of both spectral features are much larger for the photoemission geometry. When approaching the L_3 resonance position, the relative weight of the satellite increases. At resonance, both contributions are much enhanced and the intensity is now isotropic.

We denote the ground state in Ni as $[3d^9 4s]$ where the square brackets indicate that the valence electrons are in the metallic state. Taking screening into account the two types of final states may be written as $[3d^9 4s]^{-1}$ and $3d^8(X)[4s^2]$, respectively. The screening electron in the latter state is taken from the Fermi level. X is a spectroscopic assignment of the atomic $3d^8$ state. At the $2p$ thresholds we have the additional possibility to make excitations to $2p^5[3d^{10} 4s]$ states. These may decay by electron emission in Auger-like processes (autoionization). The Auger process in Ni leads to localized as well as delocalized final states [17], i.e., the same type of states as in direct photoemission.

Figure 2 shows, on a binding energy scale, spectra recorded around the $2p_{3/2}$ threshold. Below threshold, the whole spectrum stays at constant binding energy, and the shape changes as discussed above. Immediately above threshold, we observe how the 6 eV feature starts to move

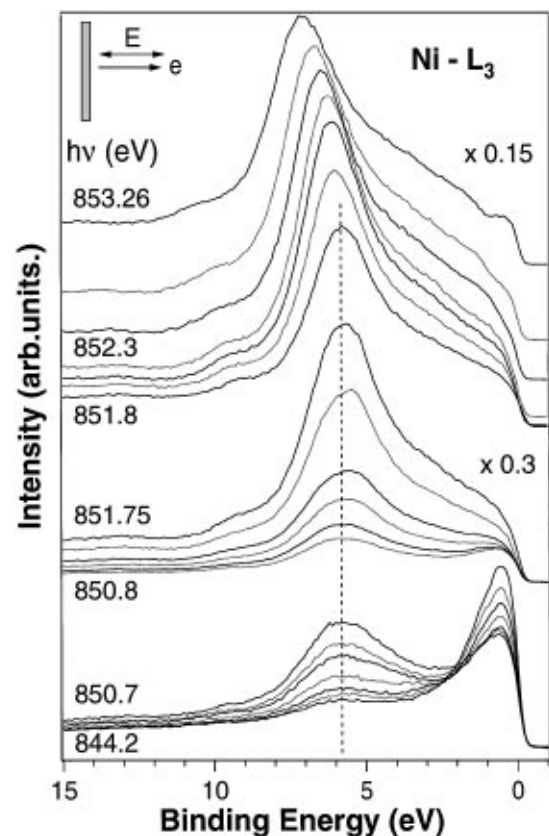


FIG. 2. Valence electron spectra around the L_3 core-level threshold (on a binding energy scale). The photon-energy increment is about 0.2 eV except for the lower set of data (844.2, 848.0, 849.0, 849.8, 850.3, 850.5, 850.7). The solid and dashed lines are as in Fig. 1.

as a function of photon energy. This indicates inelastic processes and consequently a loss of coherence [18]. In the valence-band region a weak shoulder develops from the Fermi-level cutoff and disperses with photon energy. This demonstrates the appearance of Auger-type features also in the bandlike part of the spectrum.

The kinetic energy of the $3d^8[4s^2]$ feature is plotted in Fig. 3 as a function of photon energy. Below the L_3 resonance maximum it tracks the photon energy (resonant Raman behavior). At the L_3 threshold, it transforms rapidly into a constant-kinetic-energy feature. There is a narrow transition region in which the energy positions deviate slightly from the two straight lines. There are several effects which can cause such deviations. The peak consists of several (multiplet) states, and these may be affected somewhat differently at resonance yielding modifications of the gross spectral shape and apparent peak shifts [19]. Furthermore, the finite energy spread of the photon beam may yield modified spectral shapes and apparent shifts of resonant features. When there are different resonant enhancements over the utilized excitation energy window, as, for instance, for excitations at the flanks of an absorption resonance, the effective photon energy will be different from the mean value leading to apparent shifts of photoemission-like features [3]. However, decomposition of the spectra seems to indicate that at least part of the deviation from the pure Auger-like behavior above the L_3 edge is due to a photoemission component which is resonantly enhanced as well. At the L_2 edge the same type of behavior is seen.

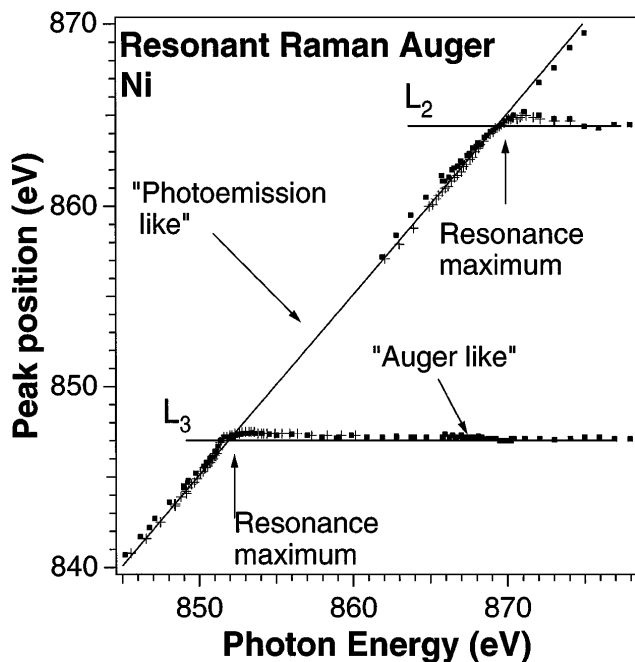


FIG. 3. The energy of the $3d^8[4s^2]$ spectral feature as a function of photon energy. Dots and crosses denote photoemission and Auger geometries, respectively.

The resonant photoemission intensity can be written

$$I(E) = 2\pi \sum_f \left| \langle f|V_r|g \rangle + \sum_m \frac{\langle f|V_A|m \rangle \langle m|V_r|g \rangle}{E_g - E_m + i\Gamma_m/2} \right|^2 \times \delta(E_f - E_g), \quad (1)$$

i.e., a sum of a direct photoemission term and a set of threshold terms [1]. The initial (g) and final (f) states contain the incoming photon and the outgoing electron, respectively, and (m) denotes the intermediate core-excited states. V_r and V_A denote the radiative and Coulomb (Auger) contributions to the interaction, respectively, and Γ_m is the lifetime width of the core-excited state.

This expression can be reformulated as a sum of the separated photoemission and autoionization intensities plus interference terms. Usually interference leads to reduced transition rates below threshold and enhanced above. Under certain conditions a standard Fano cross section, $I \approx (q + \epsilon)^2 / (\epsilon^2 + 1)$ is obtained, where $\epsilon = (E - E_{th})/\Gamma$ [1]. The square of the asymmetry parameter, q , is proportional to the ratio between the strengths of the core-level assisted (autoionization) process and the strength of the direct photoemission continuum over the core-hole width. A large q (≥ 10) corresponds to a Lorentzian-like shape, $q = 1$ gives an asymmetric Fano profile (a minimum at $\epsilon = -1$ and an equally large maximum at $\epsilon = 1$), whereas $q = 0$ gives a dip in the continuum.

Figure 4 shows the photon-energy dependence of the intensity of a region in the valence-band spectrum close to the Fermi level and for an energy window around the 6 eV satellite. The valence band intensity in the photoemission (top) and Auger (middle) geometries, respectively, reveal characteristic Fano-like dependencies. The bottom two curves (plotted together) show the intensity of the 6 eV satellite in the two geometries. At first glance there is no indication of a resonance line shape. However, the unique experimental setup which makes it possible to vary the polarization of the excitation without varying any other experimental parameter allows one to tune the relative weights of the photoemission (strong angular dependence) and autoionization (isotropic) matrix elements. Measurements for the two geometries yield differences which are characteristic of Fano profiles with different q , showing that the two channels interfere (see inset). The interference term is small only due to the dominance of the autoionization channel.

We find that the curves cannot be fitted with standard Fano line shapes. One reason for this is that the coherence is largely lost above threshold (delocalization of the intermediate state), i.e., we have a situation with several discrete states and continua. This implies that the basic assumptions for the Fano model; i.e., one discrete state and an underlying continuum is not valid. It is instructive anyway to compare the profiles to the Fano model in order to get an approximate measure of the importance of

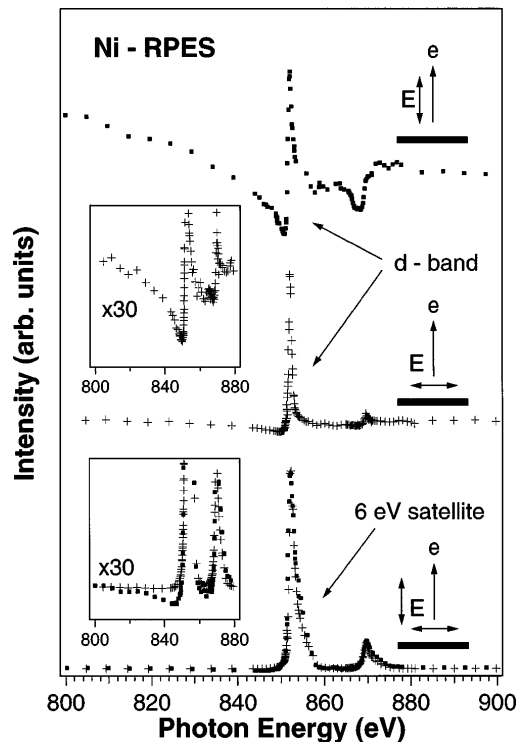


FIG. 4. Intensity of the valence-band emission and the 6 eV satellite as function of photon energy in the photoemission (dots) and Auger (crosses) geometries.

the interference in terms of the asymmetry parameter q . As seen from Fig. 4, q is smallest for the valence band, in particular, in the photoemission geometry ($q \sim 1.5$ at L_3). This channel is the majority channel in photoemission and the minority one in autoionization, yielding similar magnitudes of the matrix elements in Eq. (1). For the satellite, the opposite situation is true, and consequently much larger q values are found ($q \gtrsim 20$ and $q \sim 9$ in the Auger and photoemission geometries, respectively). Going to the L_2 edge, we find more pronounced Fano-like profiles corresponding to smaller q values (best seen for the valence band in the photoemission geometry, $q \sim 0.5$) as expected due to the weaker absorption and larger lifetime width of the L_2 level (see the definition of q above). Hence a fully consistent picture of the resonance profiles is obtained in terms of interference.

In conclusion, we find that there is indeed resonant photoemission in Ni. Interference effects are unambiguously revealed, and they explain in a consistent way the variation in the photon energy-dependent intensity profiles at the $2p$ core edges as a function of (i) whether the valence band or 6 eV satellite is considered, (ii) what core edge is used, and (iii) the polarization direction of the incident

light. At threshold, there is a transition from a resonant Raman regime with a coherent fraction around 1 to an Auger regime with a coherent fraction which rapidly drops towards zero above threshold. This result explains the observation that the resonances cannot be described by Fano profiles. In terms of the resonance behavior, the intermediate state does not appear strongly localized (other than the strong enhancement of the 6 eV satellite). This implies that Ni is not a special case and consequently that similar resonance phenomena should occur rather generally and also for systems with much more delocalized band states. The utilization of resonances at deeper core edges will thus provide a rather general method for obtaining element- and symmetry-projected density-of-states information for transition-metal systems. In particular, the utilization of the angular dependence of the resonance profiles should allow controlled studies based on this effect.

This work was supported by the Swedish Natural Science Research Council (NFR), the Göran Gustafsson Foundation for Research in Natural Sciences and Medicine, and the Swedish Institute (SI). A. L. S. is supported by the U.S. Department of Energy, under Contract No. DE-AC03-76SF00098.

- [1] C.-O. Almbladh and L. Hedin, in *Handbook on Synchrotron Radiation*, edited by E. E. Koch (North-Holland, Amsterdam, 1983), Vol. 1, and references therein.
- [2] A. Kivimäki *et al.*, Phys. Rev. Lett. **71**, 4307 (1993).
- [3] S. Aksela *et al.*, Phys. Rev. Lett. **74**, 2917 (1995).
- [4] Y. Ma *et al.*, Phys. Rev. Lett. **69**, 2598 (1992).
- [5] C. Guillot *et al.*, Phys. Rev. Lett. **39**, 1632 (1977).
- [6] U. Fano, Phys. Rev. Lett. **124**, 1866 (1961).
- [7] J. Barth, G. Kalkoffen, and C. Kunz, Phys. Lett. **74A**, 360 (1979).
- [8] M. F. López *et al.*, J. Electron Spectrosc. **71**, 73 (1995).
- [9] T. Kinoshita *et al.*, Phys. Rev. B **47**, 6787 (1993).
- [10] D. R. Penn, Phys. Rev. Lett. **42**, 921 (1979).
- [11] L. C. Davis and L. A. Feldkamp, Phys. Rev. B **23**, 6239 (1981).
- [12] G. van der Laan *et al.*, Phys. Rev. B **46**, 9336 (1992).
- [13] M. F. López *et al.*, Surf. Sci. **307-309**, 907-911 (1994).
- [14] M. F. López *et al.*, Z. Phys. B **94**, 1 (1994).
- [15] L. H. Tjeng *et al.*, Phys. Rev. Lett. **67**, 501 (1991).
- [16] N. Mårtensson *et al.*, J. Electron Spectrosc. **70**, 117 (1994).
- [17] J. Fuggle *et al.*, Phys. Rev. Lett. **49**, 1787 (1982).
- [18] O. Karis *et al.*, Phys. Rev. Lett. **76**, 1380 (1996).
- [19] An indication that this effect may be important is given by the fact that the satellite position shows a small and systematic shift between the two experimental geometries, Fig. 3. We interpret this as due to different angular dependencies for different parts of the satellite.